


# On the generation of high-quality Nyquist pulses in mode-locked fiber lasers

Yuxuan Ren(任俞宣), Jinman Ge(葛锦蔓), Xiaojun Li(李小军), Junsong Peng(彭俊松), and Heping Zeng(曾和平)

**Citation:**Chin. Phys. B, 2024, 33 (**3**): 034210. DOI: 10.1088/1674-1056/acfa87
Journal homepage: http://cpb.iphy.ac.cn; http://iopscience.iop.org/cpb

**What follows is a list of articles you may be interested in**

---

## Spatiotemporal mode-locked multimode fiber laser with dissipative four-wave mixing effect

Ming-Wei Qiu(邱明伟), Chao-Qun Cai(蔡超群), and Zu-Xing Zhang(张祖兴)
Chin. Phys. B, 2022, 31 (**10**): 104207. DOI: 10.1088/1674-1056/ac6ee9

## Generation of wide-bandwidth pulse with graphene saturable absorber based on tapered fiber

Ren-Li Zhang(张仁栗), Jun Wang(王俊), Mei-Song Liao(廖梅松), Xia Li(李夏), Pei-Wen Guan(关珮雯), Yin-Yao Liu(刘银垚), Yan Zhou(周延), Wei-Qing Gao(高伟清)
Chin. Phys. B, 2019, 28 (**3**): 034203. DOI: 10.1088/1674-1056/28/3/034203

## Mode-locked fiber laser with $MoSe_2$ saturable absorber based on evanescent field

Ren-Li Zhang(张仁栗), Jun Wang(王俊), Xiao-Yan Zhang(张晓艳), Jin-Tian Lin(林锦添), Xia Li(李夏), Pei-Wen Kuan(关珮雯), Yan Zhou(周延), Mei-Song Liao(廖梅松), Wei-Qing Gao(高伟清)
Chin. Phys. B, 2019, 28 (**1**): 014207. DOI: 10.1088/1674-1056/28/1/014207

## Observation of 550 MHz passively harmonic mode-locked pulses at L-band in an Er-doped fiber laser using carbon nanotubes film

Qianqian Huang(黄千千), Chuanhang Zou(邹传杭), Tianxing Wang(王天行), Mohammed Al Araimi, Aleksey Rozhin, Chengbo Mou(牟成博)
Chin. Phys. B, 2018, 27 (**9**): 094210. DOI: 10.1088/1674-1056/27/9/094210

## $Sb_2Te_3$ mode-locked ultrafast fiber laser at 1.93 μm

Jintao Wang(王金涛), Jinde Yin(尹金德), Tingchao He(贺廷超), Peiguang Yan(闫培光)
Chin. Phys. B, 2018, 27 (**8**): 084214. DOI: 10.1088/1674-1056/27/8/084214

---

# On the generation of high-quality Nyquist pulses in mode-locked fiber lasers

Yuxuan Ren(任俞宣)[1,†], Jinman Ge(葛锦蔓)[2,†], Xiaojun Li(李小军)[2], Junsong Peng(彭俊松)[1,‡], and Heping Zeng(曾和平)[1,3,4]

[1] *State Key Laboratory of Precision Spectroscopy, East China Normal University, Shanghai* 200062, *China*
[2] *National Key Laboratory of Science and Technology on Space Microwave, China Aerospace Science and Technology, Xi'an* 710100, *China*
[3] *Chongqing Key Laboratory of Precision Optics, Chongqing Institute of East China Normal University, Chongqing* 401120, *China*
[4] *Jinan Institute of Quantum Technology, Jinan* 250101, *China*

(Received 12 July 2023; revised manuscript received 4 September 2023; accepted manuscript online 18 September 2023)

Nyquist pulses have wide applications in many areas, from electronics to optics. Mode-locked lasers are ideal platforms to generate such pulses. However, how to generate high-quality Nyquist pulses in mode-locked lasers remains elusive. We address this problem by managing different physical effects in mode-locked fiber lasers through extensive numerical simulations. We find that net dispersion, linear loss, gain and filter shaping can affect the quality of Nyquist pulses significantly. We also demonstrate that Nyquist pulses experience similariton shaping due to the nonlinear attractor effect in the gain medium. Our work may contribute to the design of Nyquist pulse sources and enrich the understanding of pulse shaping dynamics in mode-locked lasers.

**Keywords:** mode locking, laser, soliton, fiber, pulse

**PACS:** 42.55.Wd, 42.60.Fc, 42.65.Re, 42.65.Re **DOI:** 10.1088/1674-1056/acfa87

## 1. Introduction

A Nyquist pulse is a kind of signal source that satisfies the Nyquist criterion[1] due to its zero intersymbol interference. Due to the rectangular-shaped spectrum and sinc-shaped temporal waveform, Nyquist pulses have high value in modern communication technology, from electronic communications to optical communications and ultrafast science. For example, in the field of optical communications,[2–15] Nyquist pulses can increase the bandwidth of the systems.[16] Various studies on Nyquist pulses have been reported.[17–21] Near-ideal Nyquist pulses can be generated by electrical methods with the help of an arbitrary waveform generator.[22] Due to its unmatched performance, passive mode-locking technology has developed rapidly over the past few decades.[23–26] Nyquist pulses can also be generated in passively mode-locked fiber lasers by spectral filtering effects.[19] A passively mode-locked fiber laser is a dissipative system composed of nonlinearity, dispersion, loss, gain, and a saturable absorber effect;[27] all these effects are crucial to pulse shaping in the laser. An excellent work revealed that Nyquist pulse shaping can be affected by the bandwidth and shape of the spectral filter.[19] However, it is still elusive whether other effects affect Nyquist pulse shaping in mode-locked lasers.

In this work, we demonstrate that the quality of a Nyquist pulse can be significantly affected by the dispersion, linear losses and gain in mode-locked fiber lasers. We also discover that the ideal Nyquist pulse experiences a state transition during intracavity evolution. A similariton is generated in the erbium-doped fiber (EDF) segment, and it changes into an ideal Nyquist pulse after passing the rest of the cavity.

## 2. Numerical modeling

A Nyquist pulse in the time domain is written as follows:

$$r(t)=\frac{\sin\left(\frac{2\pi t}{\tau_{\mathrm{p}}}\right)}{\frac{2\pi t}{\tau_{\mathrm{p}}}}\frac{\cos\left(\frac{2\pi\beta t}{\tau_{\mathrm{p}}}\right)}{1-\left(\frac{4\beta t}{\tau_{\mathrm{p}}}\right)^2}, \tag{1}$$

where $\tau_{\mathrm{p}}$ is the pulse duration between zero crossings, and $\beta$ is called the roll-off factor and has values in the range of 0 to 1. The sine-shaped Nyquist pulse ($\beta=0$) is an ideal pulse source due to its rectangular spectrum and zero roll-off.

Figure 1(a) depicts a schematic of the passively mode-locked fiber laser. The 1.5-m erbium-doped fiber (EDF) is the gain medium; an isolator (ISO) is employed for unidirectional operation, and a spectral filter (SF) is used for Nyquist pulse shaping. The pump power is coupled into the cavity through a wavelength division multiplexer (WDM), and the signal is coupled out using an output coupler (OC). Mode locking is realized by a nonlinear polarization rotation (NPR) device.

To give an accurate description of the pulse propagation in the cavity, we utilize the discrete model of the nonlinear Schrödinger equation (NLSE)[28]

$$\frac{\partial U}{\partial z}+\mathrm{i}\frac{\beta_2}{2}\frac{\partial^2 U}{\partial t^2}=\frac{g}{2}U+\mathrm{i}\gamma|U|^2U+\frac{g}{2\Omega_{\mathrm{g}}^2}\frac{\partial^2 U}{\partial t^2}, \tag{2}$$

†These authors contributed equally to this work.
‡Corresponding author. E-mail: jspeng@lps.ecnu.edu.cn

© 2024 Chinese Physical Society and IOP Publishing Ltd 

where $U(z,t)$ represents the slowly varying amplitude of the pulse envelope, which is the function of the propagation distance $z$ and time $t$; $\beta_2$ is group velocity dispersion (GVD). We take $\beta_2 = 65\ \mathrm{ps}^2\cdot\mathrm{km}^{-1}$ and $-22.5\ \mathrm{ps}^2\cdot\mathrm{km}^{-1}$ for the EDF and the SMF, respectively; $\gamma$ is a nonlinear coefficient, and we take $\gamma = 8\ \mathrm{W}^{-1}\cdot\mathrm{km}^{-1}$ and $\gamma = 1.5\ \mathrm{W}^{-1}\cdot\mathrm{km}^{-1}$ for the EDF and the SMF, respectively; $\Omega_g = 50$ nm corresponds to the full width at half maximum (FWHM) of the gain profile; $g$ denotes the small signal gain of the EDF, which can be expressed as

$$g = \frac{g_0}{1+\frac{E_p}{E_{sat}}}, \tag{3}$$

where $g_0 = 1800\ \mathrm{km}^{-1}$ is the small signal gain at a central wavelength of 1550 nm, $E_p = \int |U(t)|^2 \mathrm{d}t$ is the pulse energy, and $E_{sat}$ is the gain saturation energy.

The NPR device can be considered as a saturable absorber (SA), whose transmissivity is given by a monotonically increasing transfer function

$$T = \sqrt{1-q_{sat}-\frac{q_0}{\left[1+\frac{P}{P_{sat}}\right]}}, \tag{4}$$

where $P$ is instantaneous pulse power; $P_{sat}$ is the saturation power; $q$ and $q_{sat}$ are the modulation depth and the unsaturable loss, respectively.

In the cavity, the SF plays a spectral shaping role, which is crucial for Nyquist pulse shaping. After filtering, the spectrum of the amplified pulse has two sharply decreasing edges and a tunable top, which is given by

$$F(\omega) = \begin{cases} \mathrm{e}^{\alpha\frac{\omega^2}{(2\Delta\omega)^2}}, & |\omega| \le \frac{\Delta\omega}{2}, \\ 0, & \text{otherwise}. \end{cases} \tag{5}$$

In Eq. (5), $\Delta\omega$ denotes the filter bandwidth; $\alpha > 0$ ($\alpha < 0$) yields a convex (concave) Gaussian top, whose curvature is defined by the absolute value of $\alpha$. As $\alpha = 0$, the SF can be regarded as a gate function.

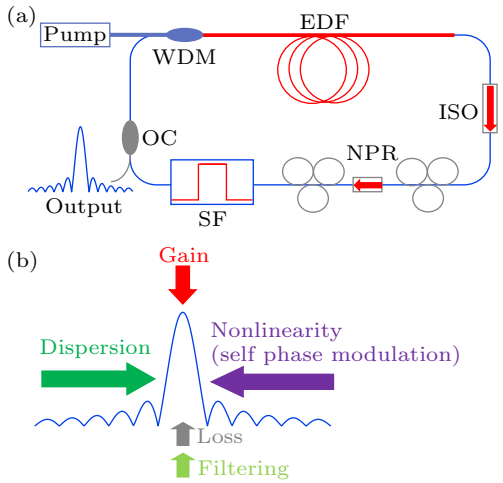



**Fig. 1.** (a) A schematic of the simulated fiber ring-cavity laser. (b) The governing law of the Nyquist pulse generation in the laser.

## 3. Simulation results and analysis

A split-step Fourier method has been employed as a numerical model.[29] The simulation starts from an initial chirp-free Gaussian pulse with a pulse width of 1 ps and peak power of 100 W centered at 1550 nm. By carefully setting the parameters, a stable sinc ($\beta \approx 0$) Nyquist pulse train can be generated after about 3000 roundtrips, as shown in Fig. 2. Specifically, we set $P_{sat} = 28$ W, $E_{sat} = 65$ pJ, and fix both parameters of the modulation depth and unsaturable loss at 0.2. A linear loss of 0.44 is considered. In addition, the net dispersion of the laser is 0.077 $\mathrm{ps}^2$, which is realized by setting the SMF length at 0.9 m. The SF's bandwidth is 7 THz ($\Delta\lambda \approx 9$ nm), and $\alpha = 0$ (Eq. (5)).

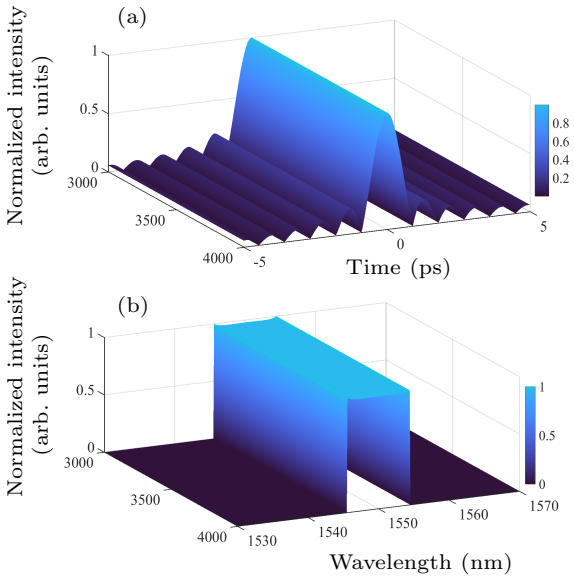



**Fig. 2.** Characteristics of the output Nyquist pulse in the time domain (a) and frequency domain (b).

### 3.1. Effects of net dispersion

Firstly, we fix the other parameters, and change the length of the SMF to investigate how the intracavity dispersion affects the properties of the generated Nyquist pulse. The simulation results are shown in Fig. 3. As we can see, together with the decrease in the fiber length from 2 m to 0.4 m, the intracavity dispersion rises up from 0.053 $\mathrm{ps}^2$ to 0.089 $\mathrm{ps}^2$, which slightly enhances the bottom oscillation of the Nyquist pulse [Figs. 3(a), 3(c) and 3(e)]. Moreover, with the increase in the total dispersion, there is an interesting phenomenon observed, where the top of the Nyquist pulse spectrum goes through a transformation from the "convex top" to the "concave top" [Figs. 3(b) and 3(f)]. Notably, in the process of the transformation, we are able to achieve a nearly sinc-shaped Nyquist pulse by controlling the fiber length, as shown in Fig. 3(d). The temporal waveform gradually approaches the ideal sinc function as the corresponding spectrums are close to flat-top.

To describe the deviation of the output pulses from the

ideal Nyquist pulse, we introduce the misfit parameter $M$,[19]

$$M^2 = \frac{|\int (|\psi|^2 - |\chi|^2) \mathrm{d}\omega|}{\int |\psi|^2 \, \mathrm{d}\omega}, \tag{6}$$

where $\psi$ is the waveform of the output pulse; and $\chi$ represents the ideal Nyquist pulse. We calculate the misfit parameter between numerical spectrums and standard rectangular fits. Here, $M = 0.0016$ for net dispersion of 0.0525 ps$^2$, $M = 0.0022$ for net dispersion of 0.0885 ps$^2$, and $M = 8.5 \times 10^{-4}$ for net dispersion of 0.07725 ps$^2$, which means the simulation is in good agreement with the theoretical fit.

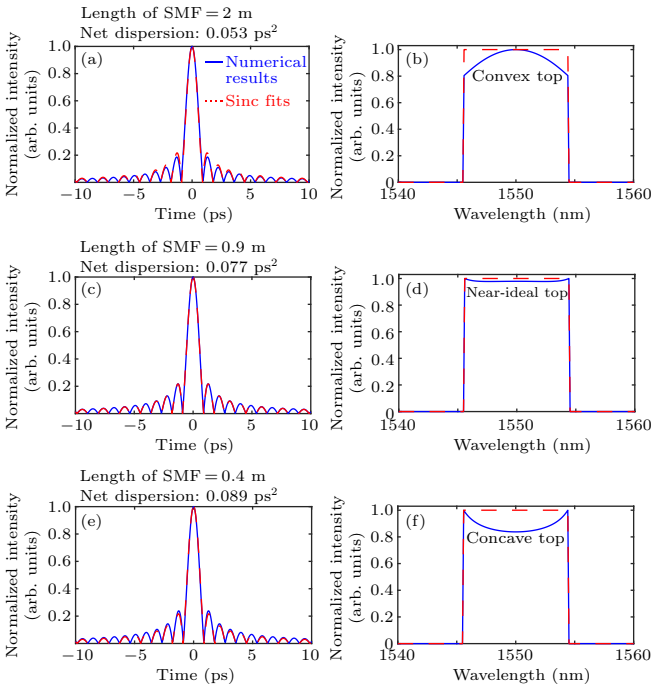



**Fig. 3.** Blue solid line: the temporal (left side) and spectral (right side) profiles of the Nyquist pulse generated under different intracavity dispersion. Red dotted line: the sinc-shaped Nyquist pulse ($\beta = 0$). [(a) and (b)] The 2-m SMF corresponds to intracavity dispersion of 0.053 ps$^2$. [(c) and (d)] The 0.9-m SMF corresponds to intracavity dispersion of 0.077 ps$^2$. [(e) and (f)] The 0.4-m SMF corresponds to intracavity dispersion of 0.089 ps$^2$.

### 3.2. Effects of cavity linear loss and gain

We also study the effects of the linear loss on the output Nyquist pulse. In the calculation, we choose three different coupling ratios of the OC (0.42, 0.48 and 0.54) to control the loss. The other parameters are the same as those used in Fig. 2. The results are shown in Fig. 4. With the increase in the intracavity loss, in the spectrum domain, a convex top shows up and has a gradually growing curvature. The misfit parameter $M = 0.0013$, $M = 9.81 \times 10^{-4}$ and $M = 6.371 \times 10^{-4}$ in Fig. 3(b), 3(d), and 3(f), respectively.

We also demonstrate the effects of the pump energy. The gain saturation energy is adjusted from 50 pJ to 75 pJ, and a similar variation trend is found as before. As shown in Fig. 5, a concave top spectrum is obtained under $E_{\mathrm{sat}} = 50$ pJ; with the growth of $E_{\mathrm{sat}}$, the top of the spectrum gradually curves in the opposite direction against the effects of linear loss.

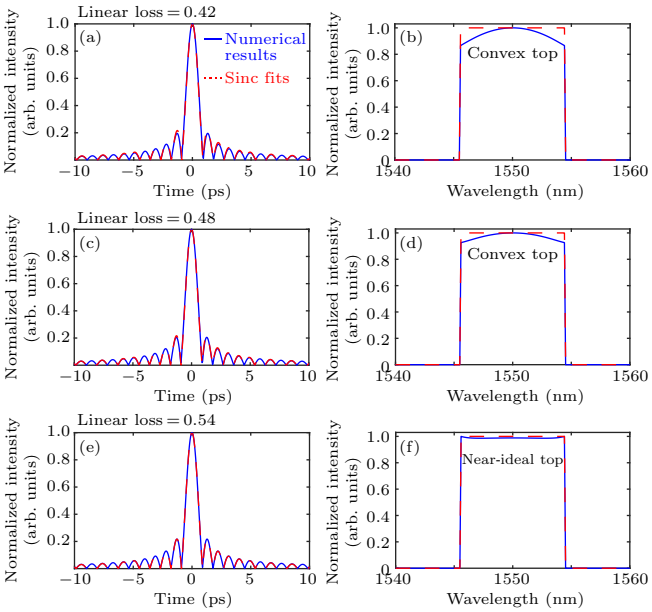



**Fig. 4.** Blue solid line: the temporal (left side) and spectral (right side) profiles of the Nyquist pulse generated under different linear losses. Red dotted line: the ideal Nyquist pulse. [(a) and (b)] Linear loss = 0.42. [(c) and (d)] Linear loss = 0.48. [(e) and (f)] Linear loss = 0.54.

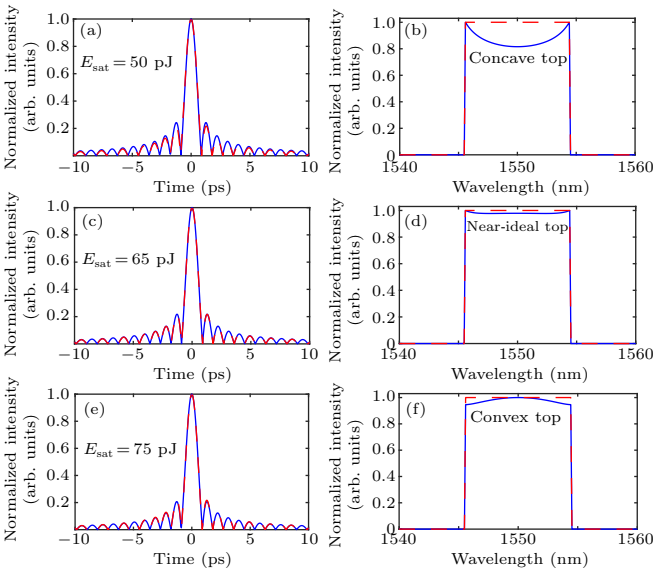



**Fig. 5.** Blue solid line: the temporal (left side) and spectral (right side) profiles of the Nyquist pulse generated under different $E_{\mathrm{sat}}$. Red dotted line: the ideal Nyquist pulse. [(a) and (b)] $E_{\mathrm{sat}} = 50$ pJ. [(c) and (d)] $E_{\mathrm{sat}} = 65$ pJ. [(e) and (f)] $E_{\mathrm{sat}} = 75$ pJ.

## 4. Similariton shaping in the Nyquist pulse laser

It has been reported that a pulse can be transformed to be a similariton[30–35] in the gain medium with normal dispersion due to the nonlinear attractor effect.[36] We also find that the Nyquist pulse becomes a similariton during the propagation in the EDF. Figure 6(a) shows the temporal evolution of the initial pulse in one roundtrip. As we can see, after the OC, we can obtain a near-ideal Nyquist pulse, as shown in Fig. 6(c).

However, the pulse in the cavity does not evolve into a Nyquist pulse directly, but undergoes a similariton shaping process in the EDF due to the above-mentioned nonlinear at-

tractor effect, as shown in Fig. 6(b). For a clear comparison, pulse waveforms after the EDF and OC are fitted via a parabolic function as a red dotted line, and a sinc function as a black dotted line, as shown in Figs. 6(b) and 6(c). It is apparent that the pulse passing through the EDF is close to being parabolic, and far away from the sinc function. By contrast, the output Nyquist pulse does not have a parabola shape.

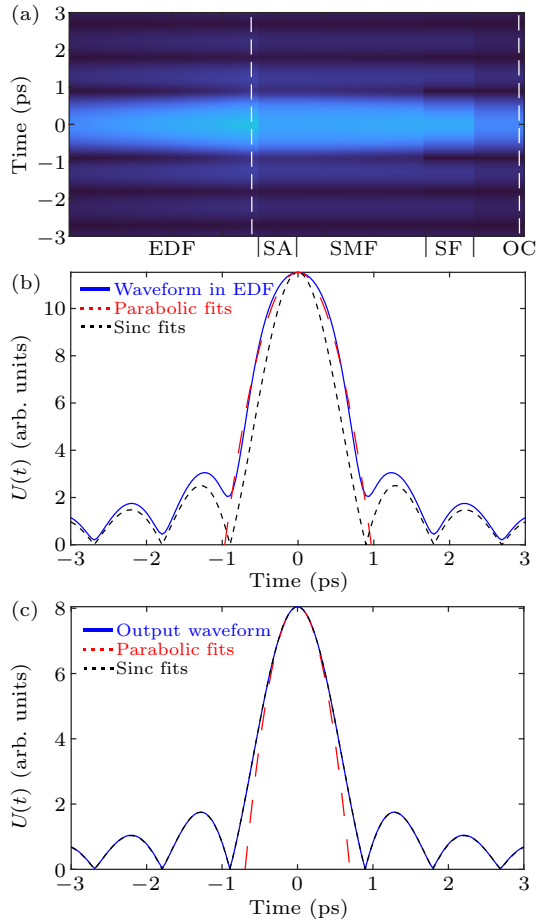



**Fig. 6.** Temporal evolution (a) of a pulse in one roundtrip. (b) The pulse waveform in the EDF. (c) The output Nyquist pulse: the red dotted line denotes parabolic fits, and the black dotted line is sinc-function fits.

## 5. Conclusion

In summary, we have numerically investigated the condition of the Nyquist pulse generation in a fiber ring-cavity laser. We find that the quality of Nyquist pulses depends on four effects: gain, dispersion, linear loss and spectral shaping. We also show that Nyquist pulses suffer from similariton shaping in the gain medium due to the nonlinear attractor effect.

## Acknowledgments

Project supported by the National Natural Science Foundation of China (Grant Nos. 11621404, 11561121003, 11727812, 61775059, 12074122, 62022033, and 11704123), Shanghai Rising-Star Program, the Sustainedly Supported Foundation by the National Key Laboratory of Science and Technology on Space Microwave (Grant No. HTKT2022KL504008), Shanghai Natural Science Foundation (Grant No. 23ZR1419000), and the National Key Laboratory Foundation of China (Grant No. 6142411196307).

## References

[1] Nyquist H 1928 *Transactions of the American Institute of Electrical Engineers* **47** 617
[2] Yue L, Kong D, Li Y and Wu J 2019 *IEEE Photon. J.* **11** 7203908
[3] Choi J, Kim J, Cho J H and Lehnert J S 2021 *IEEE International Conference on Communications*, 14–23 June, 2021, pp. 1–6
[4] Dien N V, Tuan N V, Mai L T P, Hieu N V, Phuoc V Q, Quynh N Q N and Hung N T 2022 *Computer Networks* **204** 108697
[5] Bosco G, Carena A, Curri V, Poggiolini P and Forghieri F 2010 *IEEE Photon. Technol. Lett.* **22** 1129
[6] Bosco G 2016 *Enabling Technologies for High Spectral - Efficiency Coherent Optical Communication Networks* pp. 123–156
[7] Alishahi F, Fallahpour A, Mohajerin-Ariaei A, Cao Y, Kordts A, Pfeiffer M H P, Karpov M, Almaiman A, Liao P, Zou K, Liu C, Willner A N, Tur M, Kippenberg T J and Willner A E 2019 *Opt. Lett.* **44** 1852
[8] Misra A, Kress C, Singh K, Meier J, Schwabe T, Preussler S, Scheytt J C and Schneider T 2022 *Opt. Express* **30** 13776
[9] Hirooka T, Ruan P, Guan P and Nakazawa M 2012 *Opt. Express* **20** 15001
[10] Châelain B, Laperle C, Roberts K, Chagnon M, Xu X, Borowiec A, Gagnon F and Plant D V 2012 *Opt. Express* **20** 8397
[11] Harako K, Seya D, Suzuki D, Hirooka T and Nakazawa M 2015 *Opt. Express* **23** 30801
[12] Nakazawa M, Hirooka T, Ruan P and Guan P 2012 *Opt. Express* **20** 1129
[13] Nakazawa M and Hirooka T 2021 *IEEE J. Quantum Electron.* **57** 1300320
[14] Misra A, Singh K, Meier J, Kress C, Schwabe T, Preussler S, Scheytt J C and Schneider T 2022 *Conference on Lasers and Electro-Optics (CLEO)*, 15–20, May 2022, p. 1–2
[15] Yue L, Li Y, Qiu J, Hong X, Guo H, Zuo Y and Wu J 2020 *Opt. Commun.* **455** 124362
[16] Yoshida M, Kimura K, Iwaya T, Kasai K, Hirooka T and Nakazawa M 2019 *Opt. Express* **27** 28952
[17] Soto M A, Alem M, Amin Shoaie M, Vedadi A, Brès C S, Thévenaz L and Schneider T 2013 *Nat. Commun.* **4** 2898
[18] Nakazawa M, Yoshida M and Hirooka T 2014 *Optica* **1** 15
[19] Boscolo S, Finot C and Turitsyn S K 2015 *IEEE Photon. J.* **7** 7802008
[20] Michael Yang S M 2019 *Modern Digital Radio Communication Signals and Systems*, (Cham: Springer International Publishing), pp. 113–154
[21] Xue X, Grelu P, Yang B, Wang M, Li S, Zheng X and Zhou B 2023 *Light: Science & Applications* **12** 19
[22] Schmogrow R, Hillerkuss D, Wolf S, Bäuerle B, Winter M, Kleinow P, Nebendahl B, Dippon T, Schindler P C, Koos C, Freude W and Leuthold J 2012 *Opt. Express* **20** 6439
[23] Keller U 2003 *Nature* **424** 831
[24] Han Y, Guo Y, Gao B, Ma C, Zhang R and Zhang H 2020 *Progress in Quantum Electronics* **71** 100264
[25] Ma C, Wang C, Gao B, Adams J, Wu G and Zhang H 2019 *Appl. Phys. Rev.* **6** 041304
[26] Li Y Y, Gao B, Ma C Y, Wu G, Huo J Y, Han Y, Wageh S, Al-Hartomy O A, Al-Sehemi A G, Liu L and Zhang H 2023 *Laser & Photon. Rev.* **17** 2200596
[27] Grelu P and Akhmediev N 2012 *Nat. Photon.* **6** 84
[28] Peng J and Zeng H 2019 *Phys. Rev. Appl.* **11** 044068
[29] Agrawal G P 2007 *Nonlinear Fiber Optics* (Academic press)
[30] Oktem B, Ulgudur C and Ilday F O 2010 *Nat. Photon.* **4** 307
[31] Peng J, Zhan L, Gu Z, Qian K, Luo S and Shen Q 2012 *Phys. Rev. A* **86** 033808
[32] Dudley J M, Finot C, Richardson D J and Millot G 2007 *Nat. Phys.* **3** 597
[33] Billet C, Dudley J M, Joly N and Knight J C 2005 *Opt. Express* **13** 3236
[34] Ilday F O, Buckley J R, Clark W G and Wise F W 2004 *Phys. Rev. Lett.* **92** 2139021
[35] Fermann M E, Kruglov V I, Thomsen B C, Dudley J M and Harvey J D 2000 *Phys. Rev. Lett.* **84** 6010
[36] Sidorenko P, Fu W and Wise F 2019 *Optica* **6** 1328